Inspection and structural health monitoring techniques for concentrated solar power plants

Papaelias, Mayorkinos; Cheng, Liang; Kogia, Maria ; Mohimi, Abbas; Kappatos, Vassilios ; Selcuk, Cem ; Constantinou, Louis ; Gómez Muñoz, Carlos Quiterio ; Garcia Marquez, Fausto Pedgro; Gan, Tat-Hean

DOI:
10.1016/j.renene.2015.07.090

Document Version
Peer reviewed version

Citation for published version (Harvard):
Papaelias, M, Cheng, L, Kogia, M, Mohimi, A, Kappatos, V, Selcuk, C, Constantinou, L, Gómez Muñoz, CQ, Garcia Marquez, FP & Gan, T-H 2016, 'Inspection and structural health monitoring techniques for concentrated solar power plants', *Renewable Energy*, vol. 85, pp. 1178–1191. https://doi.org/10.1016/j.renene.2015.07.090

Inspection and structural health monitoring techniques for concentrated solar power plants

Mayorkinos Papaelias[1, 3*], Liang Cheng[2], Maria Kogia[2], Abbas Mohimi[2], Vassilios Kappatos[2], Cem Selcuk[2], Louis Constantinou[1], Carlos Quiterio Gómez Muñoz[4], Fausto Pedro Garcia Marquez[4] and Tat-Hean Gan[2]

[1]ENGITEC Limited, Limassol, Cyprus
[2]Brunel Innovation Centre, Brunel University, UK
[3]School of Metallurgy and Materials, The University of Birmingham, Birmingham, UK
[4]Ingenium Group, Universidad de Castilla-La Mancha, Spain

*Contact author: Dr Mayorkinos Papaelias; E-Mail: m.papaelias@bham.ac.uk; T. +44 121 (0) 414 4060

Abstract

Parabolic trough concentrators are the most widely deployed type of solar thermal power plant. The majority of parabolic trough plants operate up to 400°C. However, recent technological advances involving molten salts instead of oil as working fluid the maximum operating temperature can exceed 550°C. CSP plants face several technical problems related to the structural integrity and inspection of critical components such as the solar receivers and insulated piping of the coolant system. The inspection of the absorber tube is very difficult as it is covered by a cermet coating and placed inside a glass envelope under vacuum. Volumetric solar receivers are used in solar tower designs enabling increased operational temperature and plant efficiency. However, volumetric solar receiver designs inherently pose a challenging inspection problem for maintenance engineers due to their very complex geometry and characteristics of the materials employed in their manufacturing. In addition, the rest of the coolant system is insulated to minimise heat losses and therefore it cannot be inspected unless the insulation has been removed beforehand. This paper discusses the non-destructive evaluation techniques that can be employed to inspect solar receivers and insulated pipes as well as relevant research and development work in this field.

Keywords: Concentrated Solar Power (CSP); non-destructive evaluation

1. Introduction

The constantly growing global energy demand coupled with the increasing effects of climate change have resulted in an urgent need for more widespread use of stable renewable sources of energy. Concentrated Solar Power (CSP) is a promising renewable energy source which can be used for predictable utility-scale power generation. From a strict techno-economic aspect, the CSP technologies which are currently commercially viable are those based on parabolic trough, Linear Fresnel Reflector and solar tower designs.

By the end of 2014 there were thirty-five CSP plants producing more than 2.5 GW of power in Europe. This represented more than 55% of the total global CSP capacity amounted to a total CSP production capacity of 4.4 GW. Outside Europe there were eleven CSP plants in the US with four of the biggest ones having been completed in 2014, three in China and twelve in the rest of the world. As of early 2015, there were twenty-two CSP plants under construction around the world which will add another 2.5 GW of capacity by 2015 (265 MW installed in Europe). Several more CSP projects have been announced around the world. If all of them materialise they will add another 9 GW of CSP capacity by 2025. At the moment, Spain is the European and world leader in the exploitation of CSP technology with the U.S.

and China following. In the U.S. the total installed CSP capacity saw a significant increase in 2014 with more than 1 GW connected to the grid. By 2020 it is anticipated that the U.S. and China will have closed the gap with Europe considerably. Nonetheless, itis expected that at least in the medium term Spain will retain its global leadership in total installed CSP capacity.

Parabolic and Linear Fresnel CSP plants consist of several km of solar absorber tubes and insulated pipes. The inspection of CSP tubing and piping is currently very challenging. In the case of solar absorbers the tubes are placed inside a glass envelope under vacuum and covered with cermet coating. The cermet coating enables a high amount of solar energy to be absorbed and very little to be reflected. The rest of the piping is insulated to minimise the total heat losses of the CSP plant and increase overall operational efficiency. To carry out any inspection in these pipes the insulation needs to be removed. The removal of pipe insulation is a time-consuming process which can potentially result in damage to both pipes and insulation.

Solar towers make use of a central absorber, where the working fluid (normally steam or molten salt) is heated by the concentrated solar rays reflected by the heliostat field directly onto the central solar absorber. Modern solar tower designs make use of volumetric solar receivers which enable much higher operational temperature and thus far higher efficiencies to be achieved in comparison to conventional parabolic-trough and Linear Fresnel CSP plants. However, the complexity of volumetric solar receivers in terms of their geometrical characteristics as well as the types of materials employed (including porous materials) poses a significant challenge to inspection engineers.

Parabolic trough and Linear Fresnel CSP plants currently suffer from operational reliability issues that are related to failures of the solar absorbers and associated coolant system piping. Failure of solar absorbers and coolant system pipes can disrupt production and result in significant maintenance costs. Mahoney of Sandia National Laboratories reported a failure rate of 30-40% in solar absorbers at the Solar Energy Generating Systems within a decade of operation [1]. The price of each solar absorber replaced was estimated to be €1000 resulting in a significant extra maintenance cost on an annual basis which was estimated to exceed €0.5 Million per annum for an average-sized CSP plant [1]. Failures can result in significant leaks and fires due to combustion of the oil commonly used as working fluid in the majority of CSP plants leading to further infrastructure damage [2].

Volumetric solar receivers used in solar towers are a more recent development. Therefore, there is limited experience in the field regarding the structural issues that may occur with time under prolonged exposure to solar radiation and high operational temperatures. The porous materials used and the complex geometry of volumetric solar receivers coupled with the lack of experience regarding the structural defects that may develop in these components with time suggest that any inspection approach other than simple visual assessment will have to be based on a trial and error approach using a portfolio of different non-destructive testing (NDT) techniques. It is evident that there is an urgent need to increase the reliability of CSP infrastructure and optimise maintenance procedures by using efficient and cost-effective inspection methods.

Although there is low technical and financial risk associated with the implementation of new parabolic trough plants in the near term, the long-term development projection has a substantially higher risk due to the technology advances needed in the fields of solar absorber efficiency, structural reliability of key plant components, thermal storage, selection of optimum working fluid and structural health assessment to enable the safe operation of the plant at temperatures above 400 °C. Existing parabolic trough plants suffer at least one week

of forced outages per year whilst solar receiver tube failure rates alone can be as high as 0.09 per tube per year [1]. With the advent of solar towers using volumetric solar receivers, novel inspection techniques will need to be developed in order to enable accurate evaluation of their structural integrity and the level of degradation experienced with time. At the moment there is no reliable methodology for the inspection of in-service solar receivers, particularly volumetric ones and insulated pipes. Therefore, CSP plant maintenance procedures are largely corrective rather than preventive.

2. Principles of Concentrated Solar Power Production

The majority of utility-scale CSP plants are either based on parabolic trough and Linear Fresnel Reflector (LFR) technology. A noteworthy number of commercial solar tower-based plants have also been constructed. However, the exact inspection methodology to be employed for volumetric solar receivers is still unclear. The commercial feasibility of dish Stirling CSP plants is yet to be proven.

All CSP plants obey to the same fundamental operational principle which is none other than the concentration of a large amount of solar rays using mirrors on a solar receiver through which the working fluid is flowing. The working fluid, oil, molten salt, steam or air, as it flows through the solar absorber tubes becomes hot. The heat gained by the working fluid, unless it is steam already, is then used to generate high-temperature steam as it goes through a heat exchanger. The steam produced is then fed to a steam turbine generating electricity [3].

If steam is used as the working fluid, then it can be fed directly to the steam turbine and thus the requirement for a heat exchanger is removed. However, the higher pressures associated with the use of direct steam necessitate the use of thicker tubes and piping in order to withstand the stresses they are exposed to.

The majority of CSP plants use oil as working fluid. Therefore, the operational temperature needs to be kept below 400°C to prevent oil decomposition and/or combustion. However, with molten salts becoming more commonplace as working fluid operating temperatures of up to 580°C are possible. Direct Steam Generation although used commercially, it is not as commonplace, since it involves higher structural risks and thus, requires thicker absorber tubes to sustain the higher wall pressures required during operation. Archimedes Solar Energy recently announced the construction of a DSG CSP plant in Brasil [4]. The operational temperature of the CSP plant is a critical parameter for the maximum power generation efficiency that can achieved.

Parabolic trough and LFR CSP plants have been so far financially viable for large utility scale power generation, where the power capacity has been larger than 50 MW. Almost all large-scale projects are currently based on these two types of technologies. A number of solar tower projects have been constructed or are currently under construction, with many more having also been announced.

The graph in Figure 1 shows the global cumulative installed CSP capacity by the end of 2014 [5]. The uptake and track record of CSP technologies up until the end of 2013 is shown in Figure 2. Parabolic trough CSP is the most established technology in terms of installed capacity.

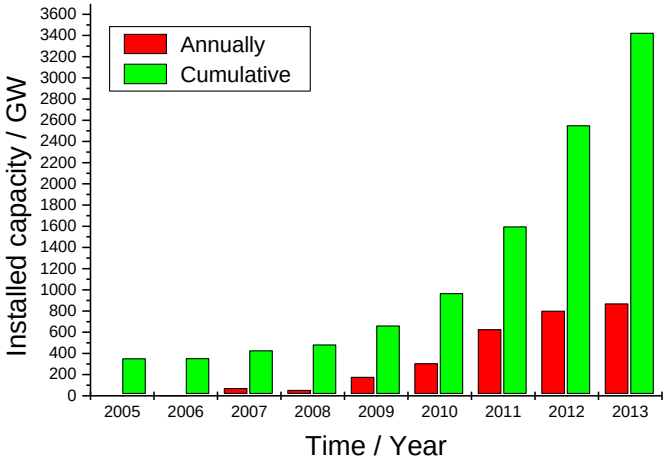

Figure 1: Global cumulative installed CSP capacity [5].

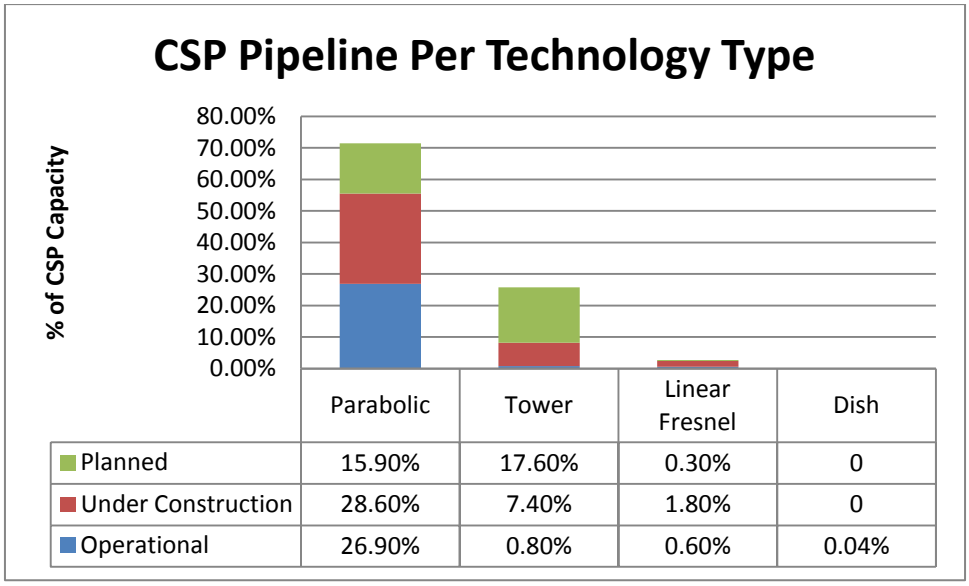

	Parabolic	Tower	Linear Fresnel	Dish
Planned	15.90%	17.60%	0.30%	0
Under Construction	28.60%	7.40%	1.80%	0
Operational	26.90%	0.80%	0.60%	0.04%

Figure 2: Implementation of CSP technologies as of 2013 [6].

Modern CSP plants are designed to operate for more than 40 years. Due to the high costs of construction of such plants Operating & Maintenance (O & M) costs need to be optimised whilst the availability and capacity factor maximised for the entire operational lifetime of the plant. The actual structural condition of solar absorber stainless steel tubes and insulated

pipes cannot be evaluated easily since the surface to be inspected is inaccessible to maintenance crews.

3. Materials for solar absorber tubes, volumetric solar receivers, insulated pipes and storage tanks

Solar absorber tubes operate under very harsh conditions. CSP plants make use of a wide range of materials for the manufacture of key structural components including plain carbon steels (cold storage tanks and secondary piping) and stainless steels (solar absorber tubes, valves, primary coolant system piping, hot storage tanks and pumps). The schematic in figure 3 shows the main features of a typical solar absorber tube.

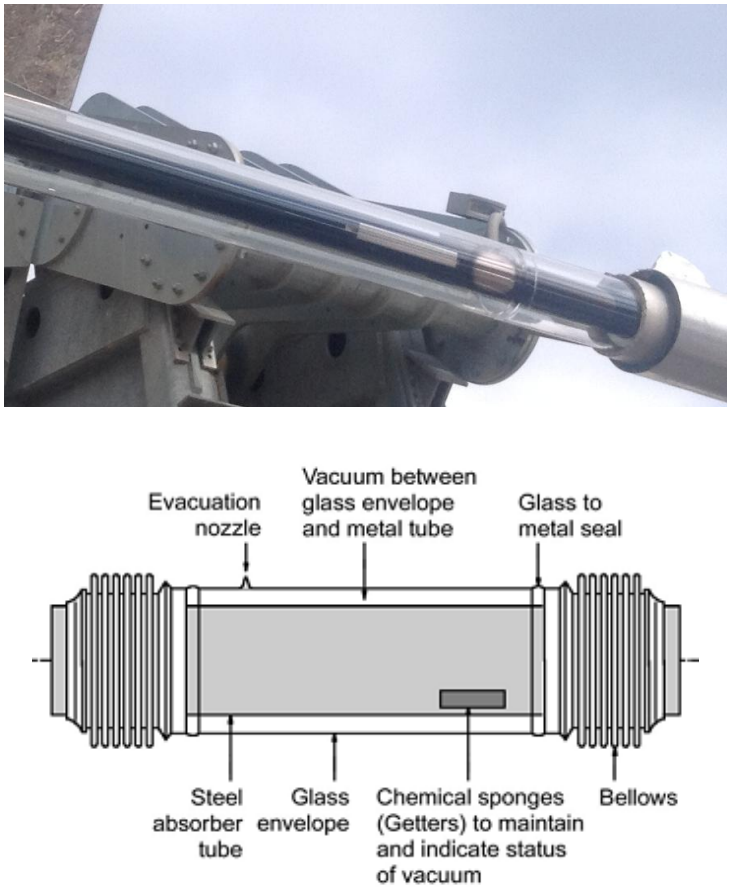

Figure 3: Typical solar absorber tube used in parabolic trough and LFR CSP plants. [schematic taken from reference 7].

The thickness and diameter of solar receiver tubes needs to be optimised to ensure the efficient heating of the working fluid. Typical commercial solar absorber tubes are manufactured of austenitic stainless steel grades such as 304L, 316Ti or 321H with an overall length of 4 m per section which are then welded together using precision orbital Tungsten Inert Gas (TiG) welding [8-10]. The typical diameter of the solar absorber tube is 70 mm. The wall thickness of the solar absorber tube depends on the working fluid employed. Normally, 1.5-3 mm wall thickness is employed for oil and molten salt-based operation and 4-6 mm for DSG. The higher wall thickness is required in DSG to withstand the higher pressures involved during operation. Bellows welded using automated electron beam welding

are employed to accommodate dimensional changes of the stainless steel tubes due to dilation and contraction during cyclic heating and cooling.

Solar absorber tubes are covered with cermet (ceramic-metal composite compound) absorber coatings and placed inside a borosilicate glass envelope. The cermet coatings need to exhibit high absorptivity and low emissivity at the operational temperature range to maximise efficiency of the CSP plant. Furthermore, they need to withstand the dimensional changes sustained by the stainless steel substrate during cyclic heating and cooling. The borosilicate glass envelope surrounding the stainless steel tube is evacuated to minimise heat losses during operation. A chemical sponge or getter is employed to maintain and indicate the vacuum status. After some time in operation the glass envelope requires evacuation to be repeated in orderto maintain heat losses at the lowest possible level. The glass envelope needs to exhibit minimum reflectivity and absorptivity and maximum transmissivity of solar rays.

It is evident that the inspection of solar absorber tubes is extremely difficult due to the complexity of their design described in detail earlier. Volumetric solar absorbers used in solar towers is also very challenging due to the ceramic or metallic porous mesh used to heat the air flowing through them. The operation of volumetric solar receivers is based on the flow of ambient (open volumetric receivers) or pressurised air (pressurised volumetric receivers) entering from the front side and flowing through the volume of the receiver picking up heat through convection.

In the pressurised design the hot air is then fed via a pipe to a gas turbine. The gas turbine drives the generator and compressor whilst the waste heat is used to drive the steam-cycle of the CSP plant increasing efficiency. In the open volumetric design, the hot air flows directly to the heat exchanger generating steam that drives the steam turbine and subsequently turns the generator in order to produce the tower. The materials used in volumetric solar receivers are subjected to temperatures that can exceed 1000 °C. Therefore the materials used in the construction of volumetric solar receivers need to be resistant to excessive heat and thermal shock.

In CSP plants the coolant system piping is insulated to minimise heat losses during plant operation as shown in Figure 4. Therefore inspection can only be carried out only after removing the insulation which is a very time consuming and expensive process.

Figure 4: The photograph shows insulated pipelines and a molten salt storage tank at PSA, Tabernas Desert, Spain.

4. Structural degradation mechanisms

The main CSP structural components, i.e. the solar absorber tubes, volumetric solar receivers and piping of coolant system are exposed to temperature and UV aging, thermomechanical fatigue, thermal shock, overheating, creep, hot corrosion, metal dusting, hydrogen embrittlement, and stress corrosion cracking.

Temperature and UV aging of the cermet coating is a common problem experienced in solar receivers used in CSP plants. Cermet coatings are generally designed to generally maintain their structural integrity as well as absorptivity and emissivity properties over the entire lifetime of the solar receiver under the design temperature range [11]. However, deviations in the operational temperature parameters due to temporary local overheating caused by variations in the flow of the working fluidand UV effects can have a detrimental effect on cermet coatings resulting in changes in the absorptivitiy and emissivity exhibited [11-13]. Gradual deterioration of the structural integrity of the cermet coating can also arised from the cyclic dilation and contraction of the substrate.

Thermomechanical fatigue of solar absorber tubes and CSP plant piping can be caused by turbulent mixing of hot and cold flow streams of the working fluid over time resulting in temperature variations across the tube or pipe wall [14]. Moreover, cyclic heating and cooling during normal operation can contribute further to the effect of thermomechanical fatigue of both the substrate metal as well as the cermet coating. Thermomechanical fatigue arises due to thermal expansion and contraction producing abnormal thermal stress loads on top of normal stresses associated with the flow of the working fluid. Thermomechanical fatigue can result in early initiation of thermal cracks followed by rapid propagation and subsequently final failure [15-17]. Plants based on DSG are generally more prone to thermomechanical fatigue-related problems. Thermal shock can occur if rapid and significant changes occur in the temperature of the solar tubes or piping. Pressurised volumetric solar receivers may exhibit thermomechanical fatigue and thermal shock. Although the air pressure is relatively low (particularly in the case of open volumetric designs) the receiver is made of porous materials which can be fairly brittle. The presence of

micro-cracks remaining after the complex manufacturing process of the honeycomb structure of the receivers can intensify the thermomechanical fatigue phenomenon. Thermal shock may also result in cracking. Accidental overheating can lead to damage of the volumetric solar receiver necessitating the replacement of the affected tiles.

Pitting and general corrosion of the solar receiver and insulated pipes is another common structural degradation mechanism. Operation at a wide temperature range involving repeated heating and cooling cycles may result in more aggressive forms of corrosion [18]. Corrosion and Stress Corrosion Cracking (SCC) can lead to sudden and catastrophic failure, especially in DSG plants operating at high pressure [19-20]. Local pitting corrosion can cause initiation of stress corrosion cracking or result in small-scale leaks. Most stainless steel pipes are vulnerable to pitting corrosion and stress corrosion cracking [21].

Interrupted or poor flow of the working fluid can cause certain solar absorber tube sections to overheat [22]. This can lead to deterioration of the structural integrity of the cermet coating and its absorptivity and emissivity properties, accelerated creep damage, thermal oxidation, softening and stress rupture of the stainless steel tube. Obstruction of the working fluid can occur due to carbon (coke) or salt deposits on tube and pipe walls with time or due to corrosion debris travelling from the CSP pipework to the solar field. The solar absorber tubes have far smaller diameters than the rest of the pipelines of the CSP plant, Moreover, the pipework in CSP plants is not necessarily manufactured from the same steel grades and therefore pipes carrying working fluid to and from the solar field can experience different corrosion rates. Large corrosion debris particles can travel with the working fluid from the pipes to the solar field occasionally blocking the flow of working fluid and resulting in overheating. Overheating can result from the presence of carbon or salt deposits even if the flow of the working fluid is not obstructed by them. Carbon and salt deposits will form an insulating boundary between the working fluid and the tube wall causing gradual overheating and subsequently failure.

Metal dusting is a corrosion mechanism which affects stainless steels operating at temperatures between 300-850 °C under carbon-supersaturated gaseous environments [23-28]. Oil is currently the most common working fluid in CSP plants which operate between 300-400 °C. The use of oil as working fluid can result in carbon (coke) accumulating on tube and pipe sections. Metal dusting once it initiates will cause significant wall thickness reduction which can eventually result in failure. The micrographs in Figure 5 demonstrate an example of metal dusting on a P5 pipe carrying oil. Hochman et al. [24] revealed the effect of M_3C metastable carbide in the initiation of metal dusting. Grabke et al. [25-26] investigated further the formation and dissociation mechanisms associated with the M_3C carbide and the break-up of surface oxide films in initiating local attack.

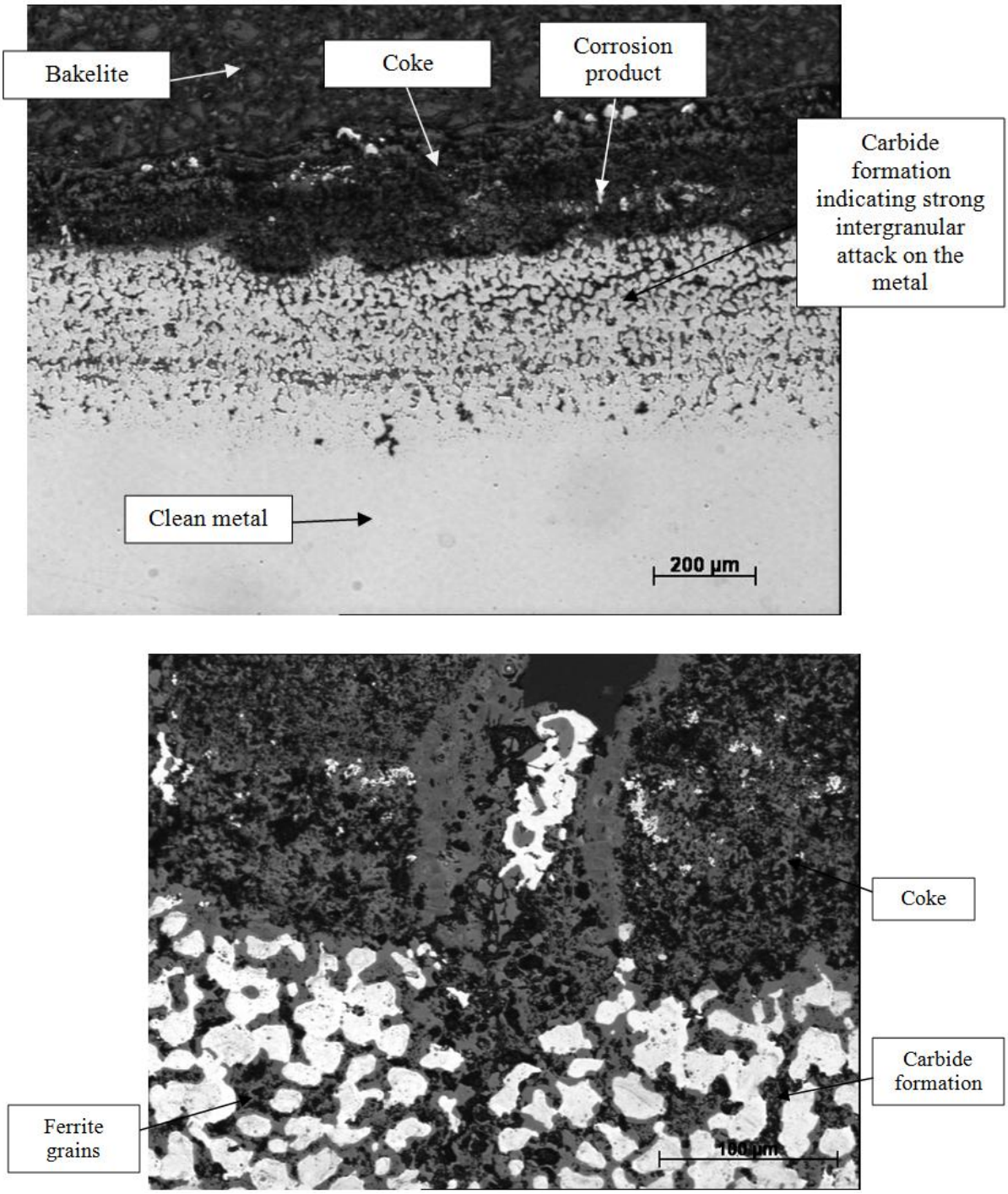

Figure 5: Metal dusting of a P5 pipe carrying oil.

Metal loss due to erosion can occur in CSP insulated pipes and solar absorbers due to internal-surface discontinuities or solid foreign objects lodged within tubes causing disturbance of the working fluid flow and increased turbulence leading to metal wasting. Erosion as a damage mechanism is of more significance to CSP plants using molten salts. However, in the case of oil-based CSP plants erosion can also influence the structural integrity of the solar absorbers tubes.

CSP pipes and solar absorber tubes may be affected by the presence of atomic hydrogen diffusing in the steel regardless of the working fluid used with the exception of air. Diffusing

hydrogen can combine at grain boundaries or inclusions in the steel to produce molecular hydrogen or react with iron carbides in the metal to produce methane. Gas accumulation can cause eventually separation of the metal at is grain boundaries causing discontinuous intergranular cracking [29].

For most CSP plants, especially those using oil as working fluid, operational temperatures do not exceed 400°C under nominal operational conditions. Hence, creep damage is not expected to be a problem unless local overheating is taking place. However, for CSP plants using molten salts or DSG as working fluids operating temperatures as high as 550 °C are possible. At this temperature creep damage becomes of importance. Thus, pipelines and solar absorber tubes will need to be evaluated for creep damage over time [30].

5. State-of-the-art Non-Destructive Evaluation techniques for CSP plants

As discussed earlier, the design of solar absorbers makes the inspection of the cermet coated stainless steel tube inside the evacuated borosilicate glass envelope very difficult with existing inspection techniques. Similarly, the inspection of insulated pipes widely used in CSP plants is very difficult unless insulation is removed. The accurate inspection of volumetric solar receivers is not at all straightforward either.

Special inspection setups can be used to inspect the tubes and pipes without having direct contact with the surface of the component of interest. However, due to the significant lift-off involved in such inspection conditions, the maximum resolution achievable is fairly low and is only appropriate for the detection of defects of considerable size. In this section, the various inspection techniques applicable for the non-destructive evaluation of key CSP structural components are discussed together with their limiting factors.

In the case of volumetric solar receivers apart from visual inspection of the surface very few techniques could be applied. One plausible approach could be the use of digital radiography including computed tomography after each tile has been removed from the field for evaluation under laboratory conditions. In the field it is doubtful that any other inspection technique other than visual observation of the tile surface can provide a meaningful result.

5.1 Visual Inspection (VI) including Automated Vision (AV)

Visual Inspection (VI) of structural components in CSP plants can offer limited information for maintenance planning. The fact that there are several kilometres of tubes and insulated piping makes VI ineffective. Furthermore, only large visible defects can be detected using this technique. VI can help assess the amount of dust on the reflectors in order to determine cleaning requirements and restore solar ray reflectivity back to optimum levels. Also damage on the supporting frames and mirrors can be assessed visually either by personnel walking through the solar field or Automated Vision Inspection (AVI) systems deployed using remotely controlled vehicles. VI may be used to detect working fluid leaks as well as damaged insulations. During outages corrosion on piping can be assessed once the insulation has been removed. The presence of fatigue cracks in the storage tanks can also be assessed visually. Internal corrosion can be assessed if the storage tanks are emptied and cleaned thoroughly before VI can be carried out. Pipe Crawling Inspection Robots (PCIR) carrying video cameras can be employed to assess the pipes internally during planned outages for the presence of visible defects before plant operation begins or after pipes have been cleaned

internally [31-33]. Visual inspection could also be used to assess volumetric solar receivers for obvious surface damage either in-situ or after removal.

5.2 Liquid Penetrant Inspection (LPI)

Liquid Penetrant Inspection (LPI) or Dye Penetrant Inspection (DPI) is a visual technique based on the use of special dyes which are spread over the area of interest for inspection, usually a weld. The dye is applied on the cleaned surface of the component to be inspected and allowed to dwell for a few minutes. Once the dye has been allowed to dwell for a sufficient amount of time the excess dye is wiped away and the developer is applied. If there is a surface defect present such as a crack or small pits then the dye that has leaked inside will flow back out after the developer has been applied providing a clear visible indication of the defect. LPI is a time consuming process carried out manually by certified inspection personnel. The technique is extremely sensitive to very small defects only a few mm in length and depth but requires thorough cleaning of the surface to be inspected before it can be used [34]. In the case of CSP plants the technique can be used to inspect welds of insulated pipes and storage tanks once the insulation has been removed as well as supporting structures of the heliostats or parabolic mirrors. The inspection is relatively fast but due to the large number of components to be inspected considerable time is required. Only surface-breaking defects are detectable with this technique. Since insulation needs to be removed, LPI can only be carried out during a planned outage. Solar absorber tubes cannot be inspected using LPI due to the presence of the glass envelope and cermet coating of the surface of the stainless steel tube. Due to the porous nature of the materials used in the manufacturing of volumetric solar receiver materials LPI is not applicable.

5.3 Magnetic Particle Inspection (MPI)

Magnetic Particle Inspection (MPI) is another visual technique based on the use of ferrous particles which are sprayed over the surface of interest. As in LPI, MPI also requires cleaning of the surface of the component to be inspected, although it does not need to be as thorough. The technique is based on the application of a magnetic field produced by a strong portable electromagnet which is used to magnetise the area of interest. Therefore, MPI is only applicable to ferrous components. If there is no defect present the ferrous particles will remain undisturbed. However, in the case of a surface-breaking or very near-surface defect magnetic flux will leak causing the ferrous particles sprayed on the surface to align in such a way that they create a visible indication of the defect present [34]. If the defect is surface-breaking and large enough a very clear visible indication is produced. However, in the case of non-surface breaking defects any indication needs to be verified using an alternative inspection technique. MPI like LPI is not applicable for the inspection of solar absorber tubes as well as piping and storage tanks manufactured from austenitic stainless steel grades. However, it is applicable to ferrous pipes used in the secondary coolant system once the insulation has been removed and the supporting structures provided that they are made of ferromagnetic steel grades. It should be noted that this technique is not appropriate for volumetric solar receivers due to the porous nature of the materials used as well as the absence of ferromagnetism.

5.4 Magnetic Flux Leakage (MFL) Inspection

Magnetic Flux Leakage (MFL) is an electromagnetic technique applicable on ferrous materials only due to the requirement of magnetising the inspected component. The application of MFL in CSP plants is limited to certain insulated ferrous pipelines, heat

exchanger tubes and cold storage tanks. MFL is not suitable for inspecting absorber tubes or insulated piping manufactured of austenitic stainless steel alloy. The technique requires sufficient magnetisation of the inspected components in order to avoid underestimating or even missing defects completely. It can be used to detect and characterise pitting and general corrosion as well cracks [35-37]. MFL inspection is affected by the relative magnetic permeability, μ_R, of the component being inspected.

Strong rare earth magnets are used to magnetise the component inspected as shown in Figure 6. If a component is free of defects the magnetic flux lines will be retained within the walls of the component. However, in the case where a defect is present some of the magnetic flux will leak. The amount of flux that will leak depends on the defect size (depth, width and length), orientation, geometry as well as the level of magnetisation achieved. The variations occurring in the induced magnetic field due to the magnetic flux leaking can be detected by an array of magnetic field sensors such as a sensing coils, Hall Effect sensors, Giant Magnetoresistance (GMR) probes or fluxgate sensors and can be related to the severity, geometry and defect [38-39]. The whole circumference of a pipe can be magnetised during inspection thus simplifying and speeding up the whole process. The spacing between adjacent sensing elements in the array must be small enough to ensure that there are no gaps across the array affecting the detection capability of the MFL system.

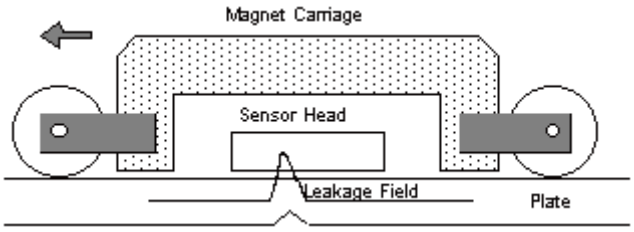

Figure 6: Schematic showing the principle of MFL [schematic taken from reference 35].

MFL is particularly suited for detection of uniform wall loss and to a lesser extent for pitting corrosion unless it is general or relatively large pits are present [40]. The inspection speed using traditional MFL method is relatively slow due to the requirement of magnetising the inspected component to a satisfactory level. Crack detection using MFL technique is orientation dependent. If a crack is parallel to the direction of the magnetising flux lines then depending also on the other geometrical parameters of the crack it may not be possible to detect it [36].

Normally, MFL inspection requires that the probe has a small lift-off no more than a few mm to be effective otherwise sufficient magnetisation and leak sensitivity drops dramatically. Therefore, inspection of insulated ferromagnetic pipes requires removal of the insulation first. The inspection process is more straightforward for the cold storage tank floor and walls as long as the tank has been emptied and cleaned beforehand. Inspection of insulated pipelines without the removal of insulation can be carried out at extremely low frequencies but with very poor resolution. A recent study in China [41] demonstrated the potential of using pulsed MFL (PMFL) to size corrosion defects on steel pipes with 20 mm insulation thickness. The sensitivity was found to be quite low at such large lift-off.

MFL can be used to inspect insulated pipes from the inside by employing intelligent pigging equipment [42]. However, this requires that the pipelines to be inspected are piggable which may not always be the case. Furthermore, the cost of inspection pigs can be quite high and

only a few inspection companies around the word offer this service. As with MPI, MFL is not applicable for the assessment of volumetric receivers either.

5.5 Eddy Current (EC) Testing

Eddy Current (EC) inspection techniques have originated from Michael Faraday's discovery of electromagnetic induction in 1831. The principle of EC is based on the phenomenon that occurs when an alternating current (AC) flows within a coil causing a changing magnetic field to be produced. If the excitation coil producing the changing magnetic field is brought near the surface of a conductor, regardless whether it is ferromagnetic or paramagnetic, will cause electric currents or eddy currents to be induced within the conductor. Depending on the frequency of the excitation AC as well as the conductivity and relative permeability of the conductor the eddy current effect may be stronger or weaker. By lowering the frequency of the excitation AC eddy currents will tend to flow at higher depths from the surface of the conductor. If higher frequencies are used (e.g. in the range of several hundreds of kHz and above) the depth that eddy currents will flow will be restricted significantly. Based on Lenz's law if there is no defect present, the induced eddy currents flowing inside the conductor will generate a secondary magnetic field which will tend to oppose the primary magnetic field created by the excitation coil. In the presence of a defect the flow of the induced eddy currents will be disturbed and hence the secondary magnetic field will fluctuate, giving rise to changes in the impedance of the sensing coil. These impedance changes can then be related to the size and nature of the defect detected [43-47]. Precise EC inspection can be a difficult task when carried out manually. In general, if high resolution is required the EC probe frequency will need to be relatively high and the size of the interrogating coil relatively small. This makes handling of the probe tricky since the resulting signal will be sensitive to lift-off effect as well as angle of the probe with respect to the surface of the component being inspected.

EC inspection can be used to detect both surface and deep structural defects as well as changes in the electrical and magnetic properties of a metal component due changes in the microstructure resulting from creep or phase changes [48]. At higher operational frequencies and depending on the conductivity and relative magnetic permeability of the material that the component is manufactured, the depth of penetration of the interrogating eddy currents will be smaller (only a few mm or less) and the inspection will be more sensitive to lift-off variations. The decrease in the magnitude of the EC signal is proportional to the cube of the lift-off. In general the lower the operational frequency, conductivity and relative magnetic permeability values the higher the depth of inspection will be. The lift-off effect will be less important as the probe frequency is reduced.

This means that at very low frequencies (1-10 Hz) and using Pulsed EC (PEC), inspection can be carried out even if substantial lift-off is involved, e.g. insulated pipelines. However, the level of resolution will be very poor as lift-off increases making possible the detection of very large defects only associated predominantly with uniform corrosion [49]. Smaller defects such as pitting corrosion or cracks will not be detectable unless the insulation is removed and higher operational frequencies are employed.

Low frequency PEC could potentially be used to assess changes in the microstructure of both the cermet coating as well as substrate of the solar absorber tube that may take place with time due to exposure at high temperatures and overheating without removing the glass envelope. Similarly, PEC can be used to evaluate insulated pipelines in CSP plants although the resolution of the inspection will be generally very low [49-50]. If the insulation is

removed PEC and Multi-Frequency Eddy Current (MFEC) testing [51] can be used to reveal cracks, pitting, corrosion and erosion in the pipes. Alternatively EC probes can be mounted on pigs and inspect the pipe from the inside. If the pipe has been emptied robotic crawlers can be used to inspect the pipe from the inside or from the outside if the insulation has already been removed. Crawlers can also be used in combination with PEC probes for the assessment of the storage tanks.

In theory, relatively low frequency pulsed eddy current testing could be used to assess thermal ageing of some metallic materials used for the manufacturing of volumetric solar receivers giving rise potentially to some useful qualitative data.

5.6 Alternating Current Field Measurement (ACFM)

Alternating Current Field Measurement (ACFM) inspection shares many similarities with conventional EC testing. An induction coil brought near the surface of a conductor induces a remote uniform alternating current field on the thin skin of the component being tested. As a result of the uniform alternating current field a magnetic field will also be generated. If there is no defect present then the AC field will remain undisturbed. However, in the presence of a defect the induced AC field will be disturbed with some of the current lines flowing around the edges of the defect and some below it. The changes in the AC field will subsequently result in variations to the associated magnetic field which can be detected using sensing coils orientated in the X and Z direction with respect to the surface being inspected. Any changes in the signal associated with the coil orientated in the X direction will be related to the depth of the defect whilst any changes associated with the coil orientated in the Z direction will be related to its length [52]. The principle of ACFM is shown in Figure 7.

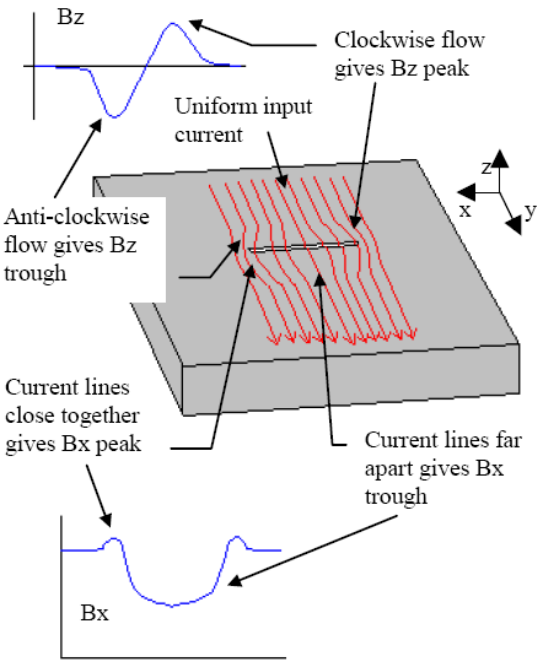

Figure 7: Definition of field directions and co-ordinate system used in ACFM [taken from reference 52].

ACFM can only be used for the detection and quantification of surface breaking defects related to corrosion and cracking. Since the decrease in the magnitude of the ACFM signal is proportional to the square of the lift-off, ACFM inspection is less sensitive to lift-off effects. Nonetheless, for lift-offs above 5 mm only considerable defects are detectable [53]. ACFM is ideal for the detection and quantification of fatigue cracks in welds particularly when no lift-of is involved in the inspection. Solar absorber tubes could, in theory at least, be inspected using ACFM probes operating at very low frequencies, however, resolution would be very poor and only the outer area of the tube would be evaluated. Similarly, insulated pipelines could be inspected but the resolution of the data would probably produce inconclusive results.

The quality of the ACFM inspection is improved dramatically if carried out after the insulation has been removed. Alternatively, ACFM probes could be mounted on pigs or robotic crawlers to carry out an internal inspection for the detection of corrosion-related defects and fatigue cracks. Furthermore, ACFM inspection can be carried out at speed with negligible changes in the resulting signal [53-54].

ACFM testing despite the similarity it has with eddy current inspection is not applicable for the inspection of volumetric solar receivers even if they are made of a conductive porous material.

5.7 Radiographic inspection

Industrial radiographic inspection can be carried out using portable X-ray or gamma ray sources. With the advent of portable fluorescence digital detectors it has become possible to replace traditional film-based radiographs with digital records [55]. Digital radiography enables the elimination of the delicate stages of film handling and developing which can sometimes accidentally induce unwanted artefacts on the film [55].

Radiography is a particularly efficient NDE method for inspecting tubing, piping and storage tanks for the presence of corrosion and weld defects [56-59]. However, radiographic inspection requires access from both sides of the inspected component, is time consuming and inherently involves serious health and safety issues.

It is obvious that it is not possible to carry out radiographic inspection throughout a CSP plant. However, it is possible to radiographically inspect components of interest where a defect is suspected or there is a risk of failure. Occasionally radiographic inspection can be carried out in order to build a statistical guide of the condition of the plant. Radiography does not require the removal of insulation from pipes. Moreover, using tangential radiographic techniques, accurate measurements of the wall thickness of pipes and tubes can be made without removing the insulation and without having to stop operation. Radiography can also be used to inspect the welds of the storage tanks during planned outages.

Digital radiography could be applied for the assessment of individual volumetric solar receiver tiles. Computed Tomography could also be used to give a three-dimensional image of the structure of the individual tiles inspected. However, this would require that the tiles are removed from the field and tested in the laboratory. This entire operation would be very time consuming, with the results and cost justification being doubtful. Nonetheless, such an inspection could be carried out on newly manufactured tiles before they are installed in the field in order to identify any micro-cracking or other defects that may be present.

5.8 Ultrasonic Testing (UT)

Conventional ultrasonic testing (UT) is based on the use of piezoelectric transducers which are capable of generating an interrogating ultrasonic beam. The transducer needs to be ultrasonically coupled on the surface of the component being inspected using a suitable couplant which is normally a water-based gel. UT can be employed for the detection and quantification of hidden and surface-breaking defects. Ultrasonic velocity measurements can be carried out to reveal microstructural changes due to phase changes or creep damage due to exposure at high operational temperatures [60-61].

Ultrasonic phased arrays consisting of several elements can increase the speed and accuracy of the inspection as well as remove some of the limitations related with the accessibility to the surface of the component since the interrogating beam can be scanned and steered in the direction of interest without having to move the probe itself. Furthermore, ultrasonic phased arrays can produce detailed C-scan images providing a useful visual record of the inspection. Two-dimensional images can be used to reconstruct three-dimensional images of the inspected component [62].

In CSP plants UT can be applied for the evaluation of pipelines and storage tanks where the insulation has been removed for the presence of cracks and corrosion. It can also be used for the inspection of supporting structures. UT probes can be mounted on pigs or robot crawlers for internal inspection of the pipes. Unfortunately, UT cannot be used for the evaluation of the solar absorber tubes due to lack of direct access on the surface of interest. The reflected time and amplitude of the ultrasound are normally monitored as features for localisation and quantification of defects. It is highly unlikely due to the nature of volumetric solar receivers that any current UT techniques could be applied for their inspection due to the technical limitations that currently exist.

5.9 Long Range Ultrasonic Testing (LRUT)

Long Range Ultrasonic Testing (LRUT) is an inspection technique which can be used to evaluate long sections of welded pipes and tubes for the presence of large cracks and corrosion in a single inspection [63-68]. The technique is particularly useful for the inspection of insulated or buried pipelines. The piezoelectric transducers can be fitted around the pipe using an inflatable ring within a small pipe length where the insulation has been removed. Thus there is no need to remove the insulation along the whole length of the pipe or excavate it if buried since only an area big enough to mount the transducer ring is required. The inflatable ring provides equal pressure on all transducers and assists ultrasonic coupling with the pipe inspected. The number of transducers employed and ring size depend on the diameter of the pipe or the tube.

LRUT uses low operational frequencies in the range of 30-200 kHz to enable the interrogating ultrasonic waves emitted from the piezoelectric transducers to travel over a long distance with minimal attenuation. The interrogating waves are able to travel over several welds before the intensity of the signal drops below the detection threshold set. The piezoelectric transducers emit interrogating ultrasonic waves towards both directions from a single location. The technique has been reported to be capable of detecting several tens of metres in either direction in a single inspection. Piezoelectric transducers used in LRUT

produce a large number of wave propagation modes travelling at different velocities. Thus, it is very important to use software which is capable of synchronising the different modes in order to produce meaningful results. Due to the low frequencies used the technique is sensitive to relatively large defects only, e.g. >5% wall thickness reduction or large transverse cracks that are able to reflect sufficient energy back to the transducers. Cracks running parallel to the direction of propagation of the ultrasonic waves are usually not detectable. In addition, LRUT inspection involves a considerably long dead zone. The dead zone is the area directly adjacent to the transducers from either direction. Since the wave front needs to become uniform in the first ~2 m of propagation due to the constructive and destructive interference of the wave fronts produced from each transducer the signal is too noisy and thus not usable. Any defects present within the dead zone will not be detectable and can interfere with the overall quality of the inspection. Another drawback in LRUT inspection is that due to the low frequencies used, interrogating waves will tend to leak in the surrounding insulation or ground reducing the signal to noise ratio and the maximum length which can be inspected in one go. If the pipe or tube is in operation during inspection then the interrogating waves can leak in the working fluid decreasing further the signal to noise ratio and subsequently the maximum resolution that can be attained becomes lower.

In CSP plants LRUT inspection can be used to assess insulated pipelines requiring insulation removal only in some locations. Furthermore, it can also be used to inspect solar absorber tubes provided that there are locations where the ring can be fitted. Unless the temperature of the tube or pipe to be inspected is below 100 °C then LRUT inspection can only be carried out during planned outages. Inherently, LRUT is not applicable for the assessment of volumetric solar receivers.

5.10 Electromagnetic Acoustic Transducers (EMATs)

Electromagnetic Acoustic Transducers (EMATs) are electromagnetic sensors capable of generating and receiving ultrasonic waves without physical contact or coupling with the surface of the component being inspected. EMATs can be used for ultrasonic inspection of both ferromagnetic and paramagnetic conductors. In EMATs the ultrasound is generated directly within the material due to magnetostriction (ferromagnetic materials) or eddy current interactions (paramagnetic but conductive materials) [69-70].

Since no coupling nor physical contact is required with the inspected component, EMATs are particularly useful for automated inspection, hot, cold, clean, or dry environments. EMATs are ideal transducers for generating Shear Horizontal (SH) bulk wave mode [71], surface waves, Lamb waves [72-74] and all sorts of other guided-wave modes in conductive and/or ferromagnetic materials. EMATs can be designed with internal cooling enabling them to operate under high temperature condition in excess of 500°C [73-74].

The Lorentz force mechanism for generation of ultrasounds in a conductor using EMATs is described next. An AC is used to excite the EMAT coil. The AC generates a changing magnetic field which induces eddy currents near the surface of the material. Due to skin effect, the distribution of the eddy current is restricted to the thin skin of the conductor. The eddy currents flowing in the magnetic field generated by the permanent magnet experience the Lorentz force causing oscillations in the materials surface which cause ultrasonic waves to be generated.

In the case of ferromagnetic materials the ultrasound generation using EMATs is caused through the magnetostrictive mechanism. Ferromagnetic materials when a strong external magnetic field is applied experience elastic deformation due to magnetostrictive effects. The strain caused due magnetostriction is dependent on the magnitude and direction of the field [70]. The high-frequency (ultrasonic scale) AC fed in the electric coil induces a changing magnetic field which causes magnetostriction in the material at ultrasonic frequency. The strain changes caused by magnetostriction subsequently result in the generation of ultrasonic waves.

In high temperature applications to avoid the problems associated with the relatively low Curie temperature of rare earth magnets, powerful electromagnets can be employed in the design of the EMAT instead. However, electromagnets are considerably large resulting in larger EMAT design. If a small EMAT is needed then the designer needs to opt for a rare earth magnet with sufficient cooling to ensure that the magnet will not degrade with time due to exposure at temperatures close to the Curie temperature or above it. Dixon et al. [74] have reported water-cooled EMATs operating at temperatures up to 450 °C which is consistent with the temperature requirements in CSP plants.

Various forms of ultrasonic waves can be easily generated using different geometries of the excitation coil and magnet/electromagnet, including Rayleigh waves. Rayleigh waves are particularly useful for detection of defects in solar absorber tubes and insulated pipes. The waves propagate along the wall thickness and thus any defect present in their path will be detectable like in LRUT. The waves are generated by electromagnetic coupling between the EMAT and the electrically conducting (and if applicable ferromagnetic) steel. EMATs are non-contact in both generation and detection modes. Lift-off of the EMAT sensors must be controlled and cannot become too large (no more than 2mm). The Rayleigh-like waves usually have frequency content in the range of 100-600 kHz. EMAT UT is not applicable for the evaluation of volumetric solar receivers as in the case of conventional UT and LRUT.

Within the INTERSOLAR project (www.intersolar-shm.com) an EMAT LRU system is currently being evaluated for the inspection of in-service solar absorber tubes and insulated pipes. The system is currently undergoing testing under laboratory conditions following completion of the numerical modelling using COMSOL. The shear horizontal EMAT used for the experimental work have been manufactured by SONEMAT Limited in the UK and are shown in Figure 8.

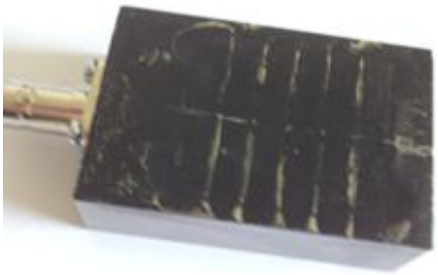

Figure 8: Photograph of one the EMATs used in the INTERSOLAR project. The EMAT was manufactured by SONEMAT Limited in the UK.

During initial evaluation trials two EMAT transducers, operating in pitch-catch mode have been mounted on a 3 mm-thick 316Ti stainless steel plate used for calibration tests. The steel grade chosen is the same grade as the one used for manufacturing absorber tubes. The photograph in Figure 9 shows the experimental set-up employed.

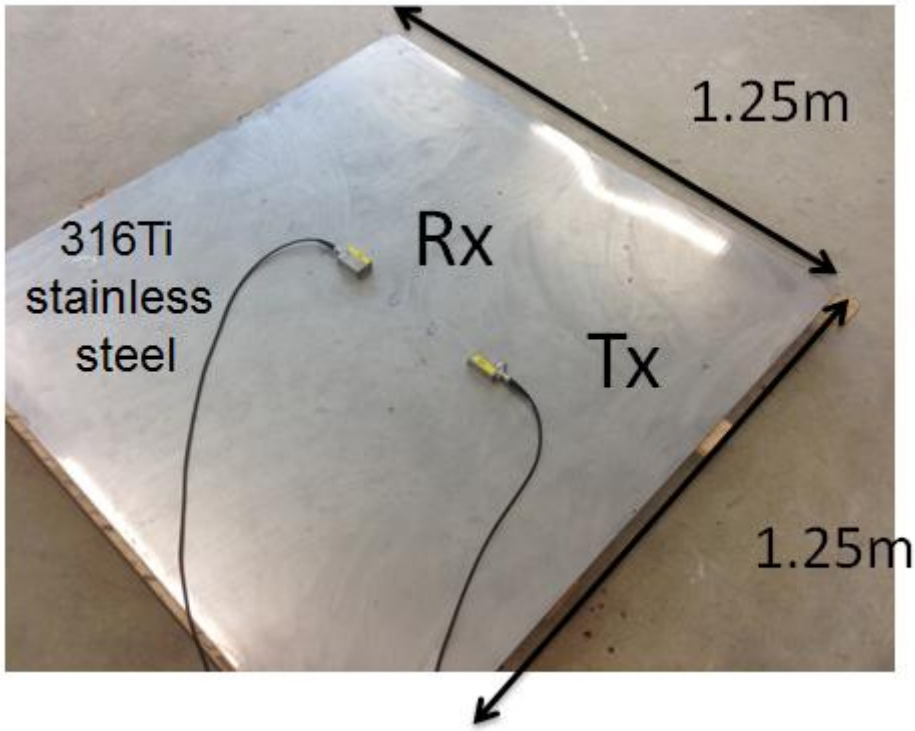

Figure 9: EMATs working in pitch-catch mode mounted on a calibration stainless steel plate.

Various artificial slot type defects simulating cracks were induced in the calibration plate. The artificially induced slots had depths from 0.5 mm to 2 mm and lengths from 13 mm to 20 mm. The EMAT transmitter was driven using a RITEC RAM-5000 system. The excitation current was modulated using a Hanning window at 256 kHz with 6 cycles and 1200 V peak-to-peak voltage.

The plot in Figure 10 shows the received signal when a crack is present between the EMAT transmitter and the EMAT receiver indicating the presence of the fault. In the plot, signal echo 1 is the pulse propagating directly from the transmitter to the receiver whilst signal echoes 2-5 are related to reflections from the boundaries of the sample plate. The signal echoes will be received regardless of whether there is a crack or not in the sample. Signal crack r1-r5 are only received when there is a crack present. This simple experiment demonstrates the capability of EMATs used in LRU testing in detecting the presence of cracks in absorber tubes. Since EMATs are non-contact and can be cooled down using a coolant such as water, they can be used to inspect solar absorber tubes continuously even when the power plant is in normal operation.

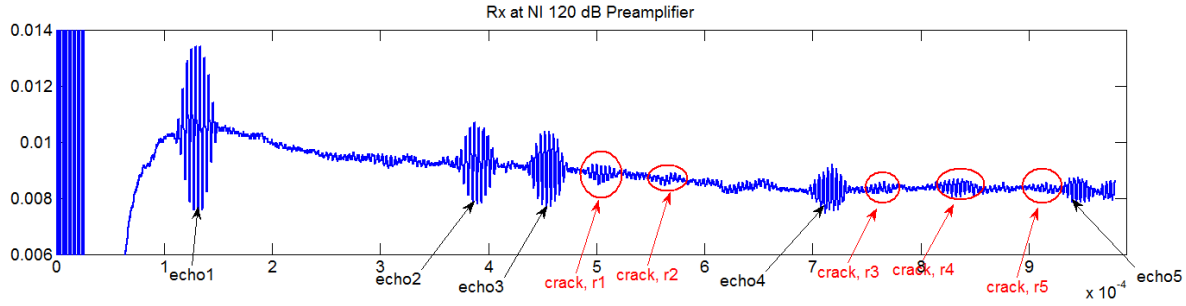

Figure 10: Raw received signal from self-develop receiver for a 2mm deep and 20mm long crack

5.11 Infrared (IR) Thermography

Inspection of CSP solar absorber tubes using infrared thermography can provide some insight regarding the overall condition of the solar field of the plant at least for identifying overheating [75]. However, due to the presence of the glass envelope and cermet coating the use of infrared cameras is not straightforward and can be unreliable unless there is clear overheating in places.

Infrared cameras are very expensive equipment ranging from 8k Euro for the simplest ones and up to 100k Euro for the most sophisticated types. There are several km of tubing in the solar field which need to be assessed. Hence, the infrared camera needs to be moved around in order to collect images for all solar receivers. Moreover, information can only be collected regarding the area of the solar absorber tube visible by the camera.

Another problem is that cermet coatings deteriorate with time resulting in variable absorptivity and emissivity at different parts of the solar field which are difficult to be identified and adjusted by the camera operator. Therefore, the infrared measurement can be prone to a significant margin of error. In addition, infrared cameras cannot be applied for the inspection of insulated pipelines as the insulation prevents direct access to the pipe's surface. However it could be used to detect damaged insulation and heat losses in the plant [76]. Infrared cameras can also be used to detect leaks as well as significant thermal variations in the tubing and piping of the plant which may indicate the presence of a potential structural problem.

Due to the thickness of the volumetric solar receivers and their porous nature, thermographic inspection would probably generate inconclusive results regarding the actual structural condition of the material. However, it could be used to evaluate the instability of air flow through the individual tiles giving a possible insight regarding problems that may exist across the structure of the individual tiles.

5.12 Acoustic Emission (AE)

Acoustic Emission (AE) is a passive but dynamic NDE technique which is extensively used for Structural Health Monitoring (SHM) by the industry. The principle of AE is based on the detection of transient elastic waves emitted when the component under evaluation is loaded up to a sufficient level to cause damage growth. AE signals are high frequency events with very small magnitude. In order to detect AE signals very sensitive piezoelectric sensors are

employed. The piezoelectric crystals convert the resulting displacement in the surface of the component to electric signals which are then suitably amplified using appropriate amplification [77-78].

AE signals can be generated from various sources including dislocation movement, plastic deformation, crack growth, corrosion, erosion, impact, friction and even phase transformation. In composite materials signals can arise from fibre debonding, delamination, matrix cracking and fibre failures. Depending on the type of damage evolution mechanism different wave types may appear. Crack growth in a metal will usually give rise to a burst type waveform. By analysing the different waveforms and other features of the AE signal it is possible to recognise the feature in the material that is giving rise to specific aspects of the recorded AE activity. In some cases depending on the extent of AE activity being recorded it is possible to assess the severity of defects present [79]. Since plastic deformation of materials is not reversible, it is necessary to know the stress history of the materials when the AE monitoring technique is employed.

Care must be given to filter unwanted noise when setting out the data acquisition parameters. A proper threshold setting is a fairly useful tool to eliminate background noise interference. Any signals of which amplitudes are below the threshold value will not be logged as AE hits. Normally, AE activity can be represented by two main types of waveforms; burst and continuous. Continuous waveforms are mainly attributed to deformation processes like cross-slip and dislocation pinning or noise and the amplitude of the signal is normally very small with relatively low duration and energy. Moreover, it is rather difficult to discriminate discrete signals from the others in a continuous waveform. Burst waveforms are often associated with events which emit higher energy such as crack initiation and propagation. In this study the useful signals are burst type and are related to crack growth or fracture. However, some burst signals are unwanted, such as echoes and need to be removed. Most of continuous waveforms captured are associated with mechanical noise or friction.

AE can detect the initiation and monitor the propagation of defects online. The information obtained about the defects detected is qualitative, i.e. their presence and potentially location can be identified, but their exact nature and severity cannot usually be ascertained easily.

In CSP plants AE can be used for SHM of storage tanks. High temperature AE sensors could be applied for the detection of corrosion debris flowing in the pipes and tubes and potentially for corrosion detection, crack initiation and propagation. Given the existing technical capabilities, it would be impossible to apply AE testing for the inspection or monitoring of volumetric solar receivers.

6 Comparison of NDE Techniques

Comparison of the advantages and disadvantages of the NDE methods available to CSP plant operators discussed earlier is shown in Table 1.

Table 1: Comparison of advantages and disadvantages of NDE methods for CSP plant inspection.

Technique	Advantages	Disadvantages	Detection capability
Visual inspection	Simple, can be automated, fast, inexpensive, can detect leaks	Provides information only regarding the surface of the component, non-	Surface defects, leaks, missing components, dust

		quantitative, cannot be applied for the inspection of solar absorber tubes and insulated piping unless insulation is removed	on mirrors
LPI	Simple, fast, high resolution, accurate, very sensitive to small surface-breaking defects, appropriate for weld inspection in pipes and storage tanks once insulation has been removed, applicable to any type of material which is non-porous	Requires surface preparation, access to the component's surface, qualitative, thorough cleaning, no permanent record, not applicable for solar absorber tube inspection and insulated pipelines, only surface-breaking defects detectable	Small surface-breaking defects such as fatigue cracks and corrosion pits
MPI	Simple, fast, high resolution, accurate, sensitive to small surface-breaking defects and larger very near-surface defects, applicable on some ferrous pipes and cold storage tanks, can be used for weld inspection	Requires some surface preparation, only ferrous materials, surface breaking and very near surface defects detectable, cannot be applied on solar absorber tubes, applicable only on ferrous piping and storage tanks once insulation has been removed	Small surface breaking and very near-surface cracks and corrosion pits
MFL	Fast, sensitive to transverse cracks and corrosion, applicable for surface and hidden defects, applicable on some ferrous pipes and storage tanks walls and floor, can be automated, low lift-off sensitivity, pigging compatible	Only ferrous pipes and storage tanks, defect geometry influences quantification, parallel cracks can be missed, if wall thickness loss is gradual can go undetected, local inspection, requires good magnetisation to avoid underestimation or missed defects, bulky equipment	Surface and hidden corrosion and fatigue cracks, inclusions
ECT	Inexpensive, sensitive to microstructural, electric and magnetic properties, sensitive to small defects, applicable to any conductive material, pigging compatible, can be automated, can operate at significant lift-offs	Very lift-off sensitive, inspection penetration depth and resolution dependent on frequency, local inspection, more efficient for surface and near-surface inspection, low resolution in high lift-offs	Surface and near-surface defects (cracks and pitting corrosion), general corrosion, microstructural changes
ACFM	Inexpensive, sensitive to small defects, capable of	Only surface-breaking defects, local inspection,	Surface-breaking defects including

	quantifying depth and length of surface-breaking defects, pigging compatible, can be automated, can operate at significant lift-offs	quantification only possible for fatigue cracks	pitting corrosion and fatigue cracks
Radiography	Accurate, does not require removal of the insulation of glass envelope, provides permanent record, can be digitised, can quantify wall loss in insulated pipes, can inspect weld quality, applicable to all components	Health and safety issues, time consuming, local inspection, requires access from both sides, bulky and expensive equipment if digital detectors and portable X-ray sources are used, very difficult to detect cracks	Internal and surface defects associated with corrosion and weld inclusions
UT	Relatively inexpensive unless phased arrays are used, capable of detecting hidden defects and quantifying both hidden and surface-breaking defects, can be applied to any type of material	Not applicable to solar absorber tubes, requires removal of insulation, local inspection	Internal and surface defects including fatigue cracks and corrosion
LRUT	Relatively fast, capable of detecting large hidden and surface breaking defects, can be applied to any type of material, can inspect long sections up to several tens of metres in one go, requires removal of insulation only in the area of installation	Only simple geometries can be inspected (i.e. pipes), considerable dead zone, defects need to be relatively large to be detectable, signal to noise ratio can be affected by the inspection conditions (e.g. presence of tight insulation, working fluid, etc.)	Relativey severe corrosion and transverse cracks
EMATs	Inexpensive, non-contact, no material limitation as long as it is conductive, can detect both hidden and surface-breaking defect, can be local or long range, can be applied at high temperature, easy to produce specific waves and modes	Low signal to noise ratio, sensor requires cooling at high temperatures, bulky sensors, lift-off cannot exceed 2 mm	Surface and hidden defects including corrosion and fatigue cracks
IR	Fast and global, excellent for the detection of heat losses, can detect leaks	Difficult to detect structural defects, can be affected by surroundings, expensive equipment	Heat losses and leak detection

AE	Continuous monitoring, can be applied for detection of crack initiation and propagation, detection of corrosion debris, long term monitoring, can be used at high temperature	No quantitative information of damage, influenced adversely by noise sources, can be expensive, complicated data management	Corrosion, cracking, leaks

Table 2 summarises the key characteristics, the main capabilities as well as the key limitations of the various NDE techniques available to CSP plant operators for the identification of defects in key structural components.

Table 2: Inspection characteristics, capabilities and limitations of the NDE techniques for CSP plants.

Inspection Characteristics	NDE Method											
	VI/AVI	LPI	MPI	MFL	ECT	ACFM	RI	UT	LRUT	EMATs	IR	AE
Detection capability	Limited (Surface only)	High (Surface only)	Average (Surface and ferrous only)	High (Ferrous only)	High (Near Surface only)	High (Surface only)	High (Corrosion only)	High (Internal and surface defects)	Average (Large defects only)	High (Internal and surface defects)	Limited (Heat losses mainly)	Average (Defect initiation and growth monitoring)
Detection resolution	Average	High	Average	Average	High	High	High (No cracks)	High	Low	Average	Low	High
Depth estimation	No	No	No	Yes	Yes	Yes	Yes	Yes	Yes	Yes	No	No
Portability/Access	High	High	High	Average	High	High	Low	High	Low	Average	High	Low
Couplant required/surface treatment/surface access	No	Yes	Yes	No	Some surface preparation may be required	No	No	Yes	Yes	No	No	Yes
Simplicity	High	High	High	Average	Average	High	Low	High	Average	Average	Average	Low
Inspection speed	Average	Average	Low	High	High	High	Low	Average	Low	High	High	Static
Appropriate for use in Pigging	No	No	No	Yes	Yes	Yes	No	Yes	No	Yes	No	No
Appropriate for use in robotic crawlers (internal or external)	Yes (AVI)	No	No	Yes	Yes	Yes	No	Yes	No	Yes	Yes	No
Level of training required	Low	High	Low	Average	High	Low	High	High	High	High	Low	High
Cost	Low	Low	Low	Average	Low	Low	High	Average	High	Average	High	High

7. Conclusions

This paper has discussed the structural issues and the potential NDT techniques which could be applied for the evaluation of solar absorber tubes, volumetric solar receivers, insulated pipes and storage tanks found in CSP plants. The structural damage affecting concentrated solar thermal power plants has been discussed in detail. State-of-the-art NDE techniques available to CSP plant operators have been compared and their advantages and disadvantages for each technique have been discussed in detail.

It is evident that CSP technology has all the credentials required to contribute profoundly in the sustainable and environmentally friendly energy production on a large scale. Nonetheless, there are still certain technical problems which need to be addressed quickly so as the long-term prospects of CSP industry are not adversely affected from excessive O & M costs and reliability issues. Further research is needed in order to develop appropriate inspection technology for the reliable assessment of critical CSP components, particularly solar absorbers and insulated pipes. With the increased use of solar tower technology, the accurate evaluation of the structural integrity of volumetric solar receivers after they are manufactured but also during their in-service lifetime will become more necessary. Therefore, research effort should be expended towards the development of new inspection techniques for such components, particularly since they are the ones responsible for harvesting the solar energy and converting it to heat.

The INTERSOLAR consortium is currently evaluating the applicability of a non-contact and non-invasive guided wave inspection platform based on EMATs for the structural health condition monitoring of solar absorber tubes and insulated pipes. Some results have been presented herewith.

Acknowledgements

The authors are indebted to the European Commission for the provision of funding through the INTERSOLAR FP7 project. The INTERSOLAR project is coordinated and managed by Computerised Information Technology Limited and is funded by the European Commission through the FP7 Research for the benefit of SMEs programme under Grant Agreement Number: GA-SME-2013-1-605028. The INTERSOLAR project is a collaborative research project between the following organisations: Computerised Information Technology Limited, PSP S.A., Technology Assistance BCNA 2010 S.L., Applied Inspection Limited, INGETEAM Service S.A., Brunel University, Universidad de Castilla - La Mancha (UCLM) and ENGITEC Limited. The authors would also like to express their sincere thanks to SONEMAT Limited for constructing the EMATs used in the project.

References

[1]. Rob Mahoney, Trough Technology Heat Collector Element (HCE) Solar Selective Absorbers, Presentation at Trough Workshop ASES 2000, June 18 2000.

[2]. MASEN preselects four groups for 500MW Moroccan solar plant, PV Magazine, http://www.pv-magazine.com/news/details/beitrag/masen-preselects-four-groups-for-500-mw-morccan-solar-plant_100001884

[3]. M. Gunther, M. Joemann, S. Csambor, Advanced CSP Teaching Materials, Chapter 5: Parabolic Trough Technology, DLR, 2011.

[4]. New direct steam generation CSP plant to be built in Brasil, CSP World, 11 November 2013.

[5]. Concentrated Solar Power Fact Book, SBC Energy Institute, June 2013.
[6]. NREL CSP projects database: http://www.nrel.gov/csp/solarpaces/by_project.cfm.
[7]. Utility scale solar power plants, a guide for developers and investors, http://www.ifc.org/wps/wcm/connect/04b38b804a178f13b377ffdd29332b51/SOLAR%2BGUIDE%2BBOOK.pdf?MOD=AJPERES
[8]. http://www.schott.com/csp/english/schott-solar-ptr-70-receivers.html?so=uk&lang=english
[9]. http://www.archimedesolarenergy.com/hems11_detailed_specifications.htm
[10]. http://www.csptube.com/Absorber_tube_specifications.html
[11]. C. E. Kennedy, Review of mid- to high-temperature solar selective absorbed materials, National Renewable Energy Laboratory (NREL) Technical Report, July 2002, NREL/TP-520-31267.
[12]. J. N. Sweet, R. B. Pettit, and M. B. Chamberlain, Optical modeling and aging characteristics of thermally stable black chrome, SEM, 10, 1984, p. 251.
[13]. H. Schellinger, M. Klank, M. Lazarov, O. Seibert, and R. Sizmann, Monitoring the aging of solar absorbers, ISES Solar World Congress, 2, 1993, p. 315.
[14]. J.L. Lee, L.-W Hu, P. Saha and M.S. Kazimi, Numerical analysis of thermal striping induced high cycle thermal fatigue in a mixing tee, Nuclear Engineering and Design, Vol. 239, Issue 5, 2009, pp. 833-839.
[15]. Y. Noguchi, H. Okada, H. Semba and M. Yoshizawa, Isothermal, thermo-mechanical and bithermal fatigue life of Ni base alloy HR6W for piping in 700 °C USC power plants, Procedia Engineering, Vol. 11, 2011, pp. 1127-1132.
[16]. G. R. Jinu, P. Sathiya, G. Ravichandran and A. Rathinam, Comparison of thermal fatigue behaviour of ASTM A 213 grade T-92 base and weld tubes, Journal of Mechanical Science and Technology, Vol. 24, No. 5, 2010, pp. 1067-1076.
[17]. S. Sunny, R. Patil and K. Singh, Assessment of thermal fatigue failure for BS 3059 boiler tube experimental procedure using smithy furnace, International Journal of Emerging Technology and Advanced Engineering, Vol. 2, Issue 8, 2012, pp. 391-398.
[18]. K. Posteraro, Thwart Corrosion under Industrial Insulation, Chem. Eng. Progress, Vol. 95, 1999, pp. 43-47.
[19]. M. Halliday, Preventing corrosion under insulation-new generation solutions for an age old problem, Journal of protective coatings & linings, Vol. 24, 2007, pp. 24-36.
[20]. F. De Vogelaere, Corrosion under insulation, Process Safety Progress, Vol. 28, 2009, pp. 30-35.
[21]. M.S. Kumar, M. Sujata, M.A. Venkataswamy, and S.K. Bhaumik, Failure analysis of a stainless steel pipeline, Engineering Failure Analysis, Vol. 15, 2008, pp. 497-504.
[22]. W. B. Stine and R. W. Harrigan, Solar energy systems design, John Wiley and Sons, Inc., New York, 1986.
[23]. C. M. Chun, J. D. Mumford, T. A. Ramanarayanan, On the mechanism of metal dusting corrosion, In the Proceedings of the High Temperature Materials Symposium in Honour of the 65th Birthday of Professor Wayne L. Worrell, Ed. S. C. Singhal, 2002.
[24]. R.F. Hochman, Proc. 4th Int. Congress on Metallic Corrosion, Ed. by N.E. Hammer, 260 NACE, 1972.
[25]. H.J. Grabke, E.M. Muller-Lorenz, E. Pippel, S. Straub, Mechanisms of Metal Dusting of Steels, In the Proceedings of UK Corrosion and EUROCORR/94, Bournemouth, 31st October – 3rd November 1994, Institute of Materials.
[26]. H.J. Grabke, R. Krajak and J. C. Nava Paz, Corrosion Science, 35, 1993, p. 1141.
[27]. H.J. Grabke, Materials and Corrosion, 49, 1998, p. 303.
[28]. T. Lant and A. B. Tomkings, Operating experience of metal dusting failures, ISBN. 01378 2001 CP, 2001.

[29]. R. D. Port and H. M. Herro, The Nalco Guide to Boiler Failure Analysis, Nalco Boiler Company, Inc. McGraw-Hill Inc., New York, 1991.
[30]. Solar materials science, Ed. L. E. Murr, Academic Press, Inc., New York, 1980.
[31]. H. T. Roman, B. A. Pellegrino, W. R. Sigrist, Pipe crawling inspection robots: an overview, IEEE Transactions on Energy Conversion, Vol. 8, Issue 3, September 1993.
[32]. Y. Kawaguchi, I. Yoshida, H. Kurumatani, T. Kikuta, Y. Yamada, Internal pipe inspection robot, In the Proceedings of IEEE International Conference on Robotics and Automation, 1995.
[33]. Y. Zhang, G. Yan, In-pipe inspection robot with active pipe-diameter adaptability and automatic tractive force adjusting, Vol. 42, Issue 12, December 2007, pp. 1618-1631.
[34]. Introduction to Non-Destructive Testing, American Society of Non-Destructive Testing Presentation, available: www.nde-ed.org/GeneralResources/IntroToNDT/Intro_to_NDT.ppt.
[35]. J. C. Drury, A. Marino, A comparison of the magnetic flux leakage and ultrasonic methods in the detection of corrosion pitting in ferrous plate and pipe, In the Proceedings of the 15th World Conference of Non-Destructive Testing, Rome, Italy, 2000.
[36]. J. C. Drury. Magnetic Flux Leakage Technology, available: www.silverwinguk.com
[37]. M. Afzal and S. Udpa, Advanced signal processing of magnetic flux leakage data obtained from seamless gas pipeline, NDT&E International, Vol. 35, Issue 7, pp. 449-457, 2002.
[38]. S. Saha, S. Mukhopadhyay, U. Mahapatra, S. Bhattacharya and G.P. Srivastava, Empirical structure for characterizing metal loss defects from radial magnetic flux leakage signal, NDT&E International, Vol. 43, Issue 6, pp. 507-512, 2010.
[39]. L. Udpa, S. Udpa and A. Tamburrino, Adaptive wavelets for characterizing magnetic flux leakage signals from pipeline inspection, IEEE Transactions on Magnetics, Vol. 42, Issue 10, pp. 3168-3170, 2006.
[40]. D. L. Atherton, Magnetic inspection is key to ensuring safe pipelines, NDT and E International, Vol. 30, p. 40, 1997.
[41]. W. Yunjiang, W. Xiaofeng, and D. Keqin, Width quantification of corrosion defect on pipeline based on pulsed magnetic flux leakage, Journal of Test and Measurement Technology, Vol. 23, pp. 390-395, 2009.
[42]. Dacon Intelligent Pigging Brochure, available at: www.dacon-inspection.com.
[43]. D. J. Hagemaier, Fundamentals of Eddy Current Testing, ASNT, 1990, ISBN 0-931403-90-1.
[44]. J. Garcia-Martin, J. Gomez-Gil, E. Vasquez-Sanchez, Non-destructive techniques based on eddy current testing, Sensors, Vol. 11, 2011, pp. 2525-2565.
[45]. J. Hansen, The eddy current inspection method, Back to Basics, available: http://www.krautkramer.com.au/the%20eddy%20current%20inspection%20method.pdf
[46]. NDT Handbook, 2nd Edition, Vol. 4 b, Electromagnetic Testing, Ed. Paul McIntyre/Mike Mester, ASNT, 1986, ISBN 0-931403-01-04.
[47]. J. M. Buckley, An introduction to eddy current testing theory and technology, available: http://www.joe.buckley.net/papers/eddyc.pdf.
[48]. M. Papaelias, Detection and measurement of phase transformation in steel using electromagnetic sensors, Ph.D. Thesis, The University of Birmingham, 2004, Birmingham, UK.
[49]. J. H. J. Stalenhoef, J. A. de Raad, P. van Rooijen, MFL and PEC tools for plant inspection, In the Proceedings of the 7th ECNDT, Copenhagen, Denmark, 26-29 May 1998.

[50]. M. A. Rogers, R. Scottini, Pulsed Eddy Current in corrosion detection, In the Proceedings of the 8th ECNDT, Barcelona, Spain, June 2002.
[51]. V. Sundararaghavan, K. Balasubramaniam, N.R. Babu and N. Rajesh, A multi-frequency eddy current inversion method for characterizing conductivity gradients on water jet peened components, NDT&E International, Vol. 38, Issue 7, pp. 541-547, 2005.
[52]. M. Lugg and D. Topp, Recent developments and applications of the ACFM inspection method and ACSM stress measurement method. In Proceedings of the 9th ECNDT, Berlin, Germany, 2006.
[53]. M. Ph. Papaelias, C. Roberts, C. L. Davis, A review of non-destructive evaluation of rail: state-of-the-art and future development, Proc. IMechE, Part F: Journal of Rail and Rapid Transit, Vol. 222, 2008, pp. 367-384.
[54]. M. Ph. Papaelias, M. C. Lugg, C. Roberts, C. L. Davis, High-speed inspection of rails using ACFM techniques, NDT & E International, Vol. 42, 2009, pp. 328-335.
[55]. Filmfree Industrial Radiography, FILMFREE FP6 Project, GA No.: NMP-2-CT-2005-515746, www.filmfree.eu.com.
[56]. T. Wawrzinek, U. Zscherpel, C. Bellon, Wall Thickness Determination in Digital Radiography, COFREND Congress on NDT, Nantes 1997, In Conference proceedings, Vol. 1, pp. 79 -83.
[57]. U. Zscherpel, C. Bellon, R. Nimtz, "Wall Thickness Estimation from Digitized Radiographs", proceedings of the 7th ECNDT, Copenhagen, Denmark, 1998, pp. 2819 – 2825.
[58]. U. Zscherpel, Y. Onel, U. Ewert, New concepts for corrosion inspection of pipelines by digital industrial radiology (DIR), In the Proceedings of the 15th WCNDT, Rome, Italy, 2000.
[59]. Ron Pincu, Digital radiography and its advantages in field NDT inspections today, In the Proceedings of the 17th World Conference on Non-Destructive Testing, Shanghai, China, 25-28 October 2008.
[60]. E. P. Papadakis, Ultrasonic velocity and attenuation: Measurement methods with scientific and industrial applications, W. P. Mason, R. N. Thurston (Eds.), Physical Acoustics, Vol. 12, Academic Press, New York, 1976, pp. 277-375.
[61]. P. Palanichamy, A. Joseph, T. Jayakumar, B. Raj, Ultrasonic velocity measurements for estimation of grain size in austenitic stainless steel, NDT & E International, Vol. 28, Issue 3, 1995, pp. 179-185.
[62]. A. Bulavinov, R. Pinchuk, S. Pudovikov, K. M. Reddy, F. Walte, Industrial application of real-time 3D imaging by sampling phased array, In the Proceedings of the 10th ECNDT, Moscow, Russia, June 2010.
[63]. M. G. Silk, K. F. Bainton, The propagation in metal tubing of ultrasonic wave modes equivalent to Lamb waves, Ultrasonics, Vol. 17, 1979, pp. 11-19.
[64]. J. L. Rose, J. J. Ditri, A. Pilarski, K. Rajana, K. and F. T. Carr, A guided wave inspection technique for nuclear steam generator tubing, NDT & E International, Vol. 27, 1994, pp307-330.
[65]. D. N. Alleyne, M. J. S. Lowe and P. Cawley, The reflection of guided waves from circumferential notches in pipes, ASME J Applied Mechanics, Vol. 65, 1998, pp. 635-641.
[66]. D. N. Alleyne, B. Pavlakovic, M. J. S. Lowe, P. Cawley, Rapid long range inspection of chemical plant pipework using guided waves, In the Proceedings of WCNDT, Rome, 2000.

[67]. P. Cawley, Practical long range guided wave inspection – applications to pipes and rail, In the Proceedings of NDE 2002, National Seminar of ISNT, Chennai, 5-7 December 2002.
[68]. J. Mu, L. Zhang, J. L. Rose, Defect circumferential sizing by using long range ultrasonic guided wave focusing techniques in pipe, Vol. 22, Issue 4, 2007, pp. 239-253.
[69]. R. B. Thomson, Chapter 4: Physical principles of measurements with EMATs, Ultrasonic measurement methods, Academic Press, New York, 1990.
[70]. M. Hirao and H. Ogi, EMATs for Science and Industry, Kluwer Academic Publishers, 2003.
[71]. M. Hirao and H. Ogi, An SH-wave EMAT technique for gas pipeline inspection, NDT & E Int., Vol. 32, No. 3, 1999, pp. 127–132.
[72]. S. Dixon and S.B. Palmer, Wideband low frequency generation and detection of Lamb and Rayleigh waves using electromagnetic acoustic transducers (EMATs), Ultrasonics, Vol. 42, 2004, pp. 1129–1136.
[73]. J. E. Bobbin, EMAT - High-temperature probe electromagnetic acoustic transducer, Mater. Eval., Vol. 37, No. 5, 1979, p. 28.
[74]. S. Dixon, C. Edwards, J. Reed, and S. B. Palmer, Using EMATs to measure the wall thickness of hot galvanizing kettles, Insight, Vol. 37, No. 5, 1995, pp. 368–370.
[75]. M. Pfander, E. Lupfert, P. Pistor, Infrared temperature measurements on solar trough absorber tubes, Solar Energy, Vol. 81, Issue 6, May 2007, pp. 629-635.
[76]. G. Jin, D. Xu, F. Pan, T. Liu, Application of infrared thermographic technique in detecting thermal loss of petrochemical thermal equipment, Infrared Technology, 2009-11.
[77]. A. G. Beattie, Acoustic emission principles and instrumentation, Journal of acoustic emission , Vol. 2, Issue 12, 1983, pp. 95-128.
[78]. Acoustic emission testing, Basics for research – Applications in Civil Engineering, Eds. C. Gross, M. Ohtsu, Springer, 2008, ISBN: 978-3-540-69895-1.
[79]. A. Berkovits, D. Fang, Study of fatigue crack characteristics by acoustic emission, Engineering Fracture Mechanics, Vol. 51, Issue 3, June 1995, pp. 401-409 and 411-416.